

A distributed model of runoff generation in the permafrost regions

L.S. Kuchment*, A.N. Gelfan, V.N. Demidov

Water Problems Institute of Russian Academy of Sciences, 117735 Gubkin 3 Moscow, Russia

Received 1 July 1999; revised 21 March 2000; accepted 21 August 2000

Abstract

A physically based distributed model of snowmelt and rainfall runoff generation in the permafrost regions has been developed. The model describes snow cover formation and snowmelt, thawing of the ground, evaporation, basin water storage dynamics, overland, subsurface and channel flow. An important feature of the model is taking into account influence of the depth of thawed ground on water input, water storage and redistribution of water input between surface and subsurface flow. The choice of the structure of the model is based on the analysis of the long-term observations of the runoff generation processes at the Kolyma water balance station and is orientated to the available standard hydrometeorological information in the cold regions. A case study of the proposed model has been performed for the Upper Kolyma River basin (the catchment area is 99,400 km²). © 2000 Elsevier Science B.V. All rights reserved.

Keywords: Distributed modelling; Runoff; Permafrost region, Model calibration/verification; River Kolyma

1. Introduction

The permafrost regions cover approximately one-quarter of the land surface of the world, more than 60% of Russia and one-half of Canada. Because of small density of population, expensive access, and limited human activity, these regions have a sparse and extremely unevenly distributed hydrometeorological network. The extensive collection of field measurement data during the last decades has considerably increased the available information on the hydrometeorological processes in the cold regions but most of these data are too fragmentary. As a result, the peculiarities of permafrost hydrology have been investigated weakly. At the same time, the growth of economical activity in the northern areas, the problem of protection of the northern environment, and also an

increasing attention to studies associated with the global processes make investigation of permafrost hydrological processes and especially runoff generation highly important and urgent. For this reason, there is much interest in developing models of the hydrological processes in permafrost regions. However, in spite of significant progress in modelling separate hydrological processes (snow cover formation and snowmelt, freezing–thawing of the ground, infiltration into frozen soil), the attempts to construct a detailed physically based model of the hydrological cycle and runoff generation for these regions met with a little success. At the same time, the comprehensive physically based models of runoff generation developed for the temperate regions can not be applicable to the permafrost river basins because of essential differences in the main processes and the lack of adequate hydrometeorological data and basin characteristics.

In this work, we have tried to construct a distributed

* Corresponding author. Fax: +7-095-1355415.

E-mail address: kuchment@mail.ru (L.S. Kuchment).

model of runoff generation in the permafrost regions based on available experience of modelling runoff generation processes in different geographical zones as well as on use of the unique hydrometeorological data collected at the Kolyma water balance station. The observations of runoff generation have been carried out at this station on seven representative basins with the drainage areas from 0.3 to 21.2 km² since 1948. The data collected for the period of these observations include the standard meteorological records, measurements of solar radiation, snow cover characteristics, soil moisture and snow evaporation, temperature and moisture of the ground, levels of ground water, runoff, chemical content of runoff. The model describes snow cover formation and snowmelt, thawing of the ground, evaporation, basin water storage dynamics, overland, subsurface and channel flow. An important feature of the model is taking into account influence of the depth of thawed ground on water input, water storage and redistribution of water input between surface and subsurface flow. A case study of the proposed model has been performed for the Upper Kolyma River basin in which the Kolyma water balance station is situated. This river basin (the catchment area is 99,400 km²) is typical of the major part of the Russian permafrost region from the point of view of both runoff generation and availability of hydrometeorological data.

2. Specific features of permafrost hydrology

The permafrost regions embrace a wide range of geological, topographical and vegetation conditions. The plain and mountainous regions of the High Arctic have barren areas with patchy tundra vegetation; parts of these areas are occupied by glaciers. The Middle and Low Arctic have tundra cover mixed with patches of barren ground. The southern part of the permafrost zone is mainly covered by boreal forests mixed with wetlands and barren mountainous areas. However, the hydrology of the permafrost regions has several common well-expressed peculiarities which make it clearly distinguishable from the hydrology of other geographical zones. According to Woo (1990), these peculiarities are the following: (1) the frozen ground has limited permeability; (2) most hydrological activities are confined to the seasonally frozen and thawed

zone above the permafrost table (the active layer); (3) energy and water fluxes are closely linked as water storage and redistribution are modified by freeze–thaw events; (4) snow and ice storage on a seasonal or multi-annual basis affects the temporal distribution of water. In the tundra areas, the open space and the strong winds lead to significant sublimation and redistribution of snow (Pomeroy and Jones, 1996; Pomeroy et al., 1997). As a result, the areal snow distribution is extremely non-uniform and snow is accumulated mainly in topographic depressions, ravines, river valleys. In the taiga area, the snow cover is distributed more evenly and has low density. Because of small permeability of frozen ground, runoff losses are determined by evaporation and water storage in depressions, peat mats, large-pored soils. The value of free basin storage capacity depends on the antecedent hydrometeorological conditions of the current year or foregoing years. The year-to-year change in basin water storage can account for 10% of the annual precipitation (Woo, 1990). The water retained on the catchment surface and in the ground can form icings (naleds) which cover considerable areas. According to Grigoriev and Sokolov (1994), in the north–east part of Russia the icings occupy 7–10% of catchment area and accumulate 200–300 mm of water. During snowmelt the main mechanism of runoff generation is the overland flow. A part of the melt water can re-freeze in the snow, in the peat mats or in the ground during the nightly lowering of air temperature and because of the low ground temperatures. The water frozen in the surface basin storage and in the active layer of the ground can generate a significant portion of river runoff during the entire warm period. There are the river basins where floods occur as a result of ice melting after cessation of snowmelt (Sokolov, 1975). Subsurface flow starts after the beginning of the icemelt in the ground and can become the main mechanism of rainfall runoff generation on the mountainous slopes. At the same time, in the northern wetlands the subsurface flow remains insignificant during the entire summer because of the high specific retention of the peat and the low hydraulic gradients (Roulet and Woo, 1986; Price and Woo, 1988). Most of the annual runoff in permafrost regions is of ice and snowmelt origin but in the southern regions rainfall runoff can dominate. Typical values of the runoff ratio are from 0.8–0.9 at the beginning of snowmelt to 0.2–0.3 at the middle of the

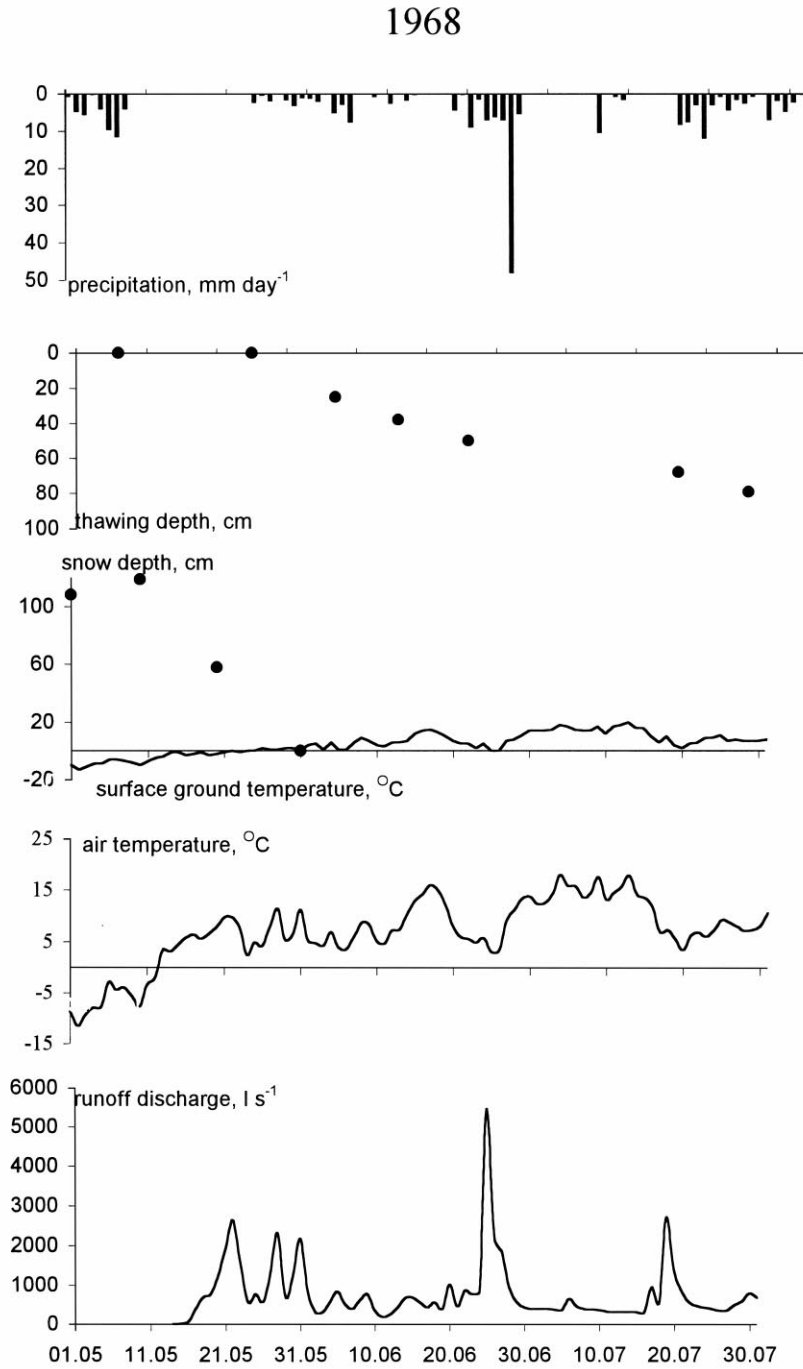


Fig. 1. Daily precipitation, depth of ground thawing, snow depth, daily surface ground temperature, air temperature, and river runoff discharge (the Kolyma water balance station; 1 May–31 July 1968).

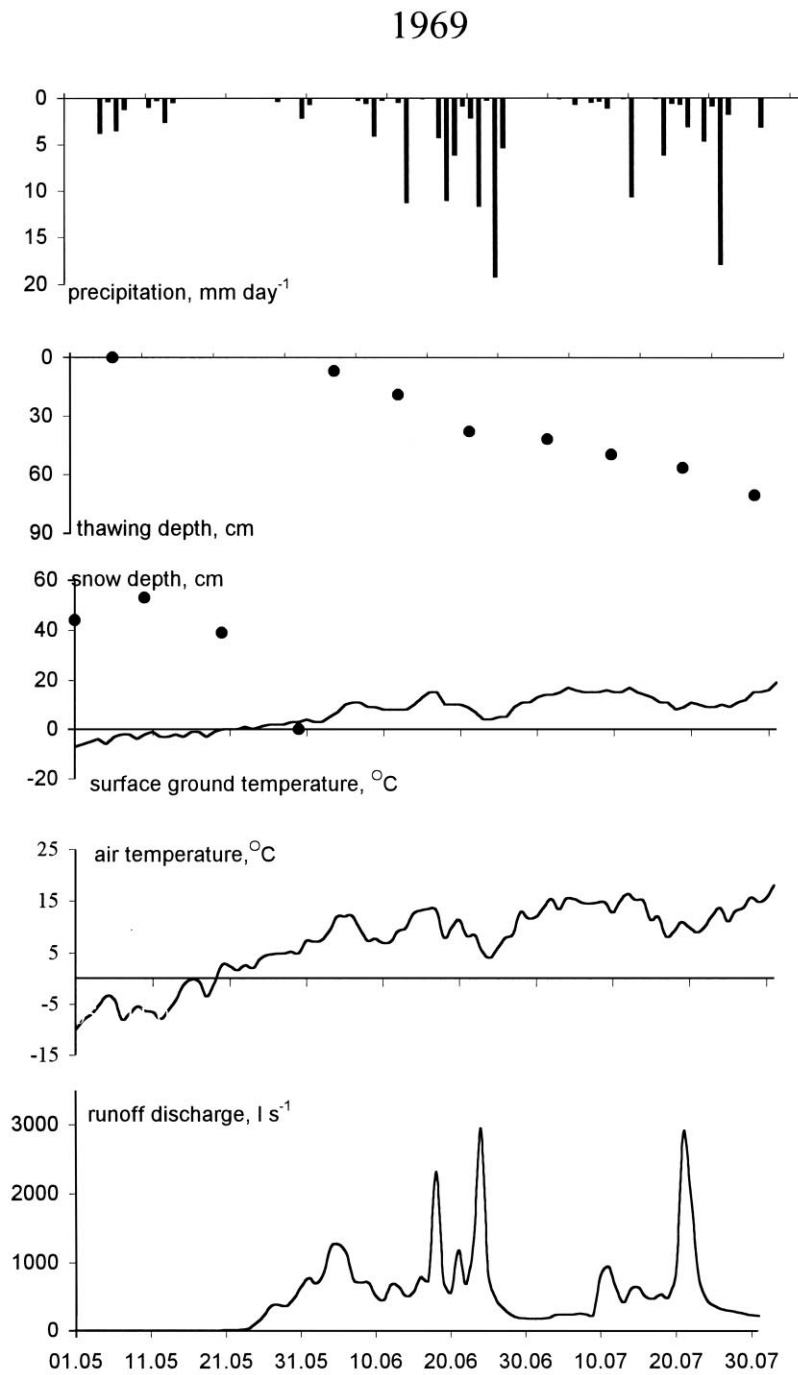


Fig. 2. Daily precipitation, depth of ground thawing, snow depth, daily surface ground temperature, air temperature, and river runoff discharge (the Kolyma water balance station; 1 May–31 July 1969).

1970

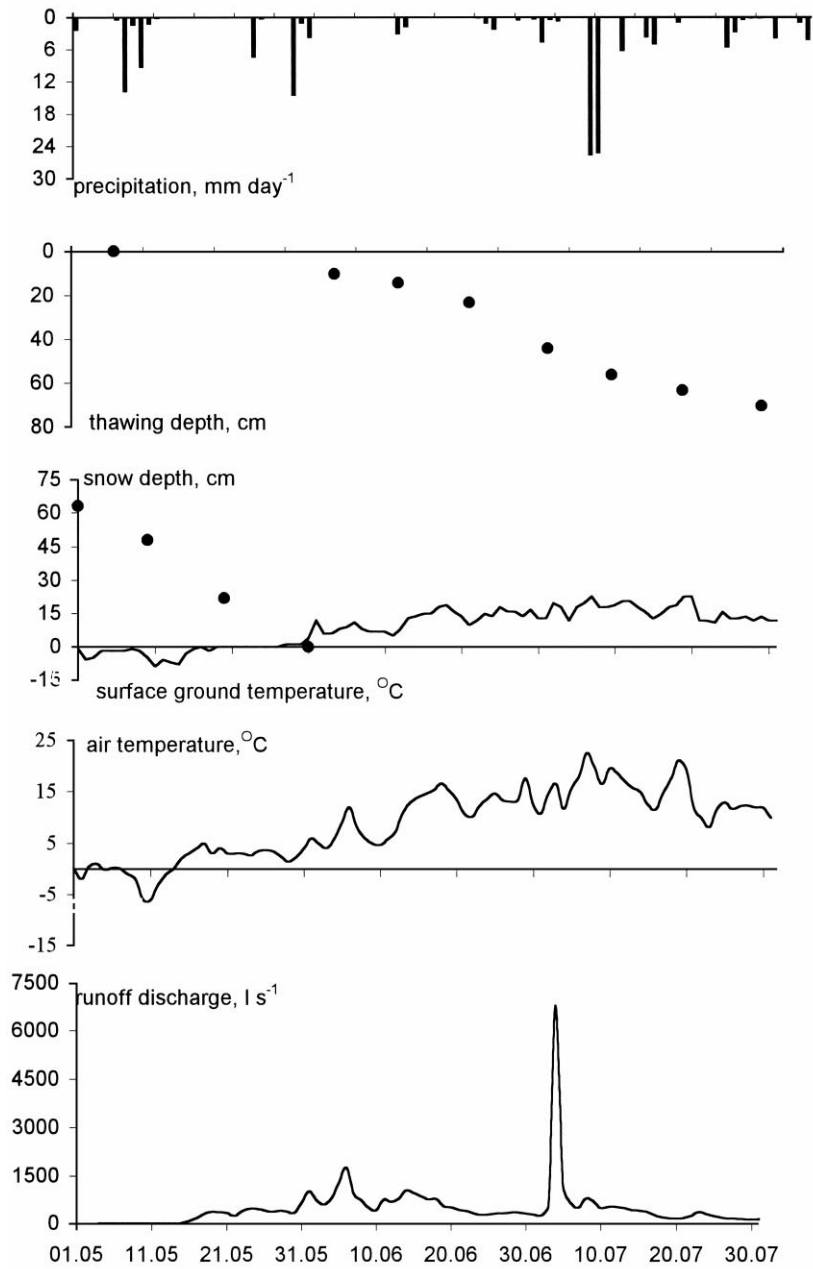


Fig. 3. Daily precipitation, depth of ground thawing, snow depth, daily surface ground temperature, air temperature, and river runoff discharge (the Kolyma water balance station; 1 May–31 July 1970).

1971

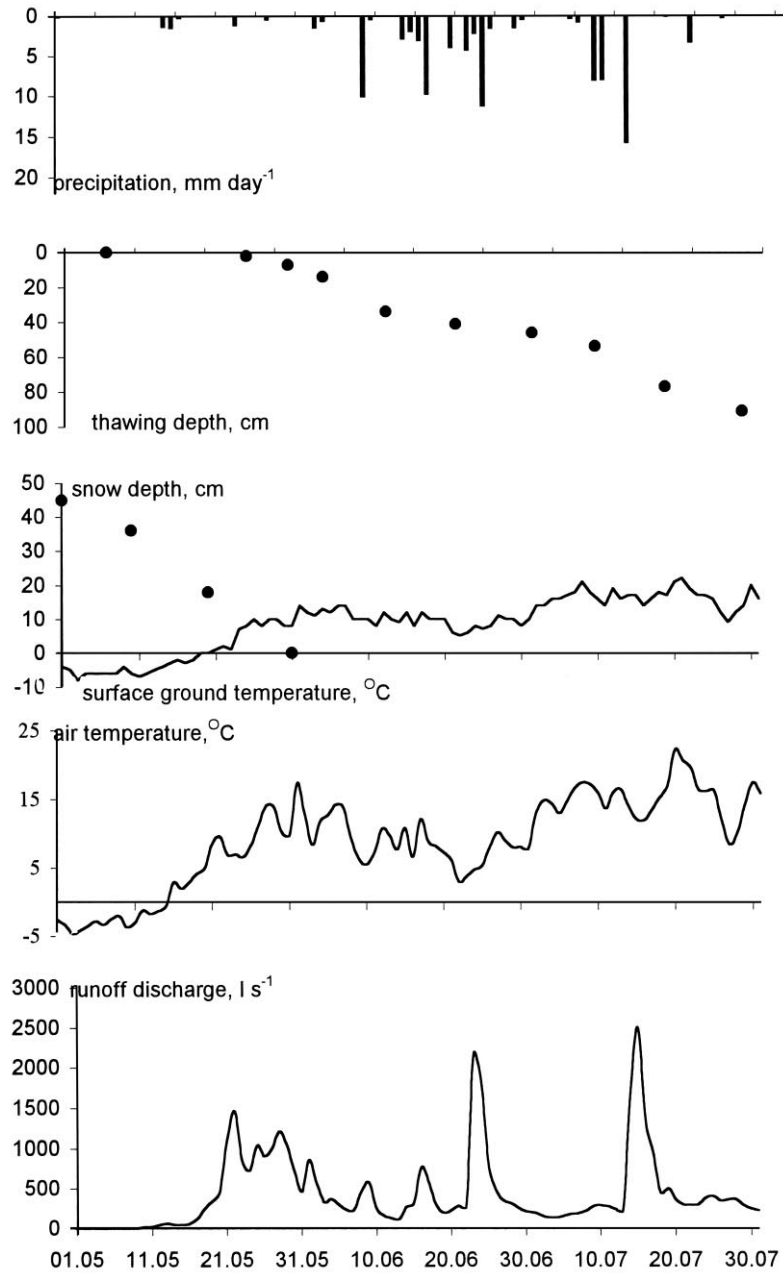


Fig. 4. Daily precipitation, depth of ground thawing, snow depth, daily surface ground temperature, air temperature, and river runoff discharge (the Kolyma water balance station; 1 May–31 July 1971).

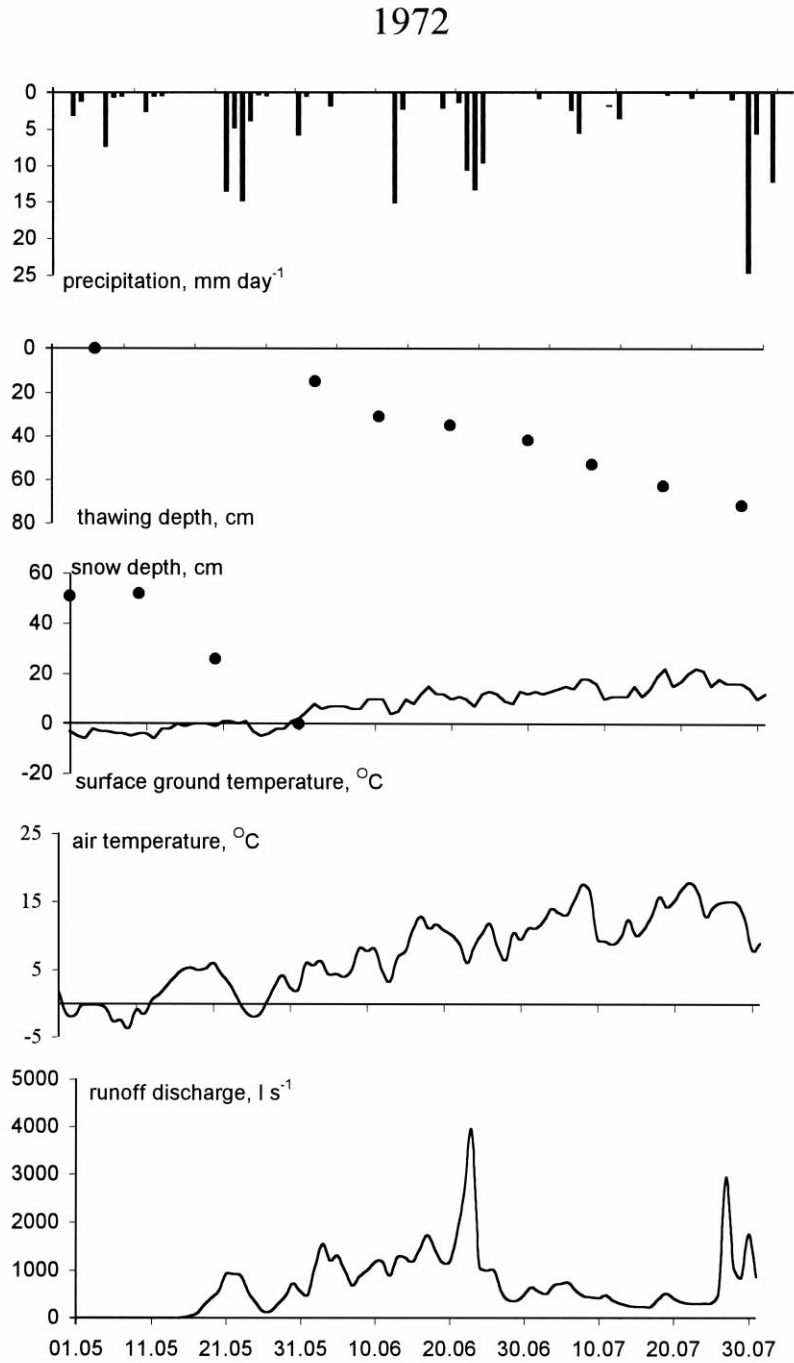


Fig. 5. Daily precipitation, depth of ground thawing, snow depth, daily surface ground temperature, air temperature, and river runoff discharge (the Kolyma water balance station; 1 May–31 July 1972).

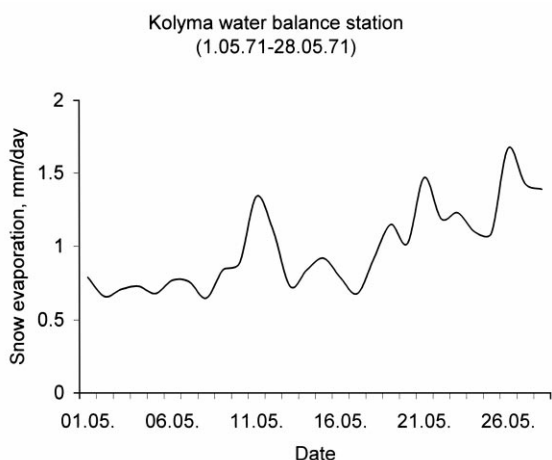


Fig. 6. Snow evaporation measured during snowmelt season in the Kolyma water balance station.

warm period when the evaporation rate becomes relatively high (Sokolov, 1975; Roulet and Woo, 1988).

The ground water component of river runoff in the permafrost regions is usually small (less than 10%), however, a rise or a lowering of water-table can play an important role in expanding or shrinking overland flow contributing areas (Roulet and Woo, 1988).

3. Landscape, climate and runoff generation mechanisms of the Upper Kolyma River basin

The Upper Kolyma River basin is located from 60 to 63°N and is a part of the Yana–Chukotka mountain country. The elevations of the river basin vary from 1000–1200 m in river valleys to 1700–2000 m at mountainous ridges. The major part of the basin is occupied by tundra and taiga. A significant part of mountainous slopes is the barren ground.

The climate is continental. The average temperature of the coldest month (January) is -34°C , the average temperature of the warmest month (July) is $+13^{\circ}\text{C}$. The period with the stable temperatures below 0°C lasts from October to April. Annual precipitation increases with the area elevation from 250 to 400 mm. About 70% of precipitation falls during the warm period. Rainfalls have usually long duration and small rates. The permanent snow cover is formed at

the beginning of October. Snowmelt begins in the middle of May.

The river basin is situated in the zone of continuous permafrost interrupted only by taliks under the river beds. The dominant soils are coarse-grained mountain-tundra podzols with large content of gravels. The peatlands occupy about 2% of the basin area. The depth of the active layer is controlled by elevation, exposure, vegetation, and presence of rivers and lakes. At the slopes of north exposure, the average depth of the active layer is 0.2–0.8 m; at the slopes of south exposure, the average depth of the active layer reaches 1.5–3.0 m.

To estimate influence of different hydrological processes on runoff generation, we have analysed the data of 20-years (1965–1984) hydrometeorological records in the Kontakny River basin (the catchment area is 21.2 km^2) situated in the Kolyma water balance station area. Figs. 1–5 show the daily air and surface ground temperatures, the daily precipitation, the snow depth, the depth of ground thawing and the river runoff measured from May to July during 5 years (1968–1972).

As can be seen from Figs. 1–5, during the entire period of records, the daily temperature of the surface layer of the ground during snowmelt was below 0°C and as a result the melting water could freeze on the ground surface or in the ground. The accumulated ice began to melt at the air temperature about $8\text{--}10^{\circ}\text{C}$ when a significant portion of the catchment area became snow-free. The snow evaporation during the snowmelt varies within a narrow range (see a typical variation in Fig. 6). During all 20 years the rise of snowmelt floods happened 3–14 days later of the snowmelt start. The maximum runoff discharges occurred when the subsurface ice melt was going (it can be seen from comparison between hydrographs and time-series of ground thawing depths in Figs. 1–5). In the case of absence of rainfalls, the hydrographs at this period follow the temporal changes of the air temperature (this effect is most pronounced in Figs. 1 and 4).

The runoff ratios during the snowmelt period are about 0.3, then at once after cessation of the snowmelt (usually the first half of June), the ratio begins to increase to 0.9 on average. At the end of summer, the runoff ratio decreases to 0.4–0.5. This temporal dynamics of the runoff ratio and analysis of the soil

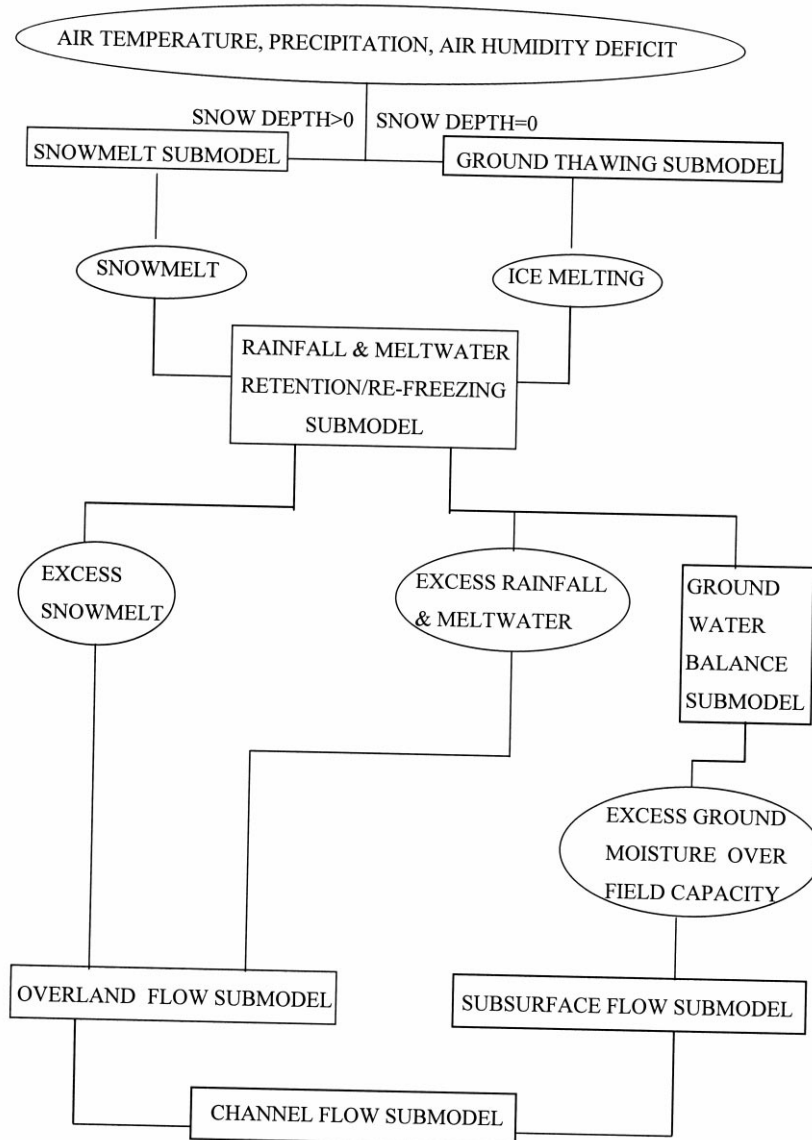


Fig. 7. Schematic diagram illustrating the major components of the model.

ice content measurements confirm the hypothesis that a considerable part of snowmelt water freezes again and reaches the river channel network only after the beginning of the ground ice melting.

A comparison of runoff hydrographs, snowmelt graphs and hyetographs reveals that the lag between peaks of water contribution and corresponding hydrograph peaks increases during the warm period from

several hours to 3–4 days. It can be explained by change of the proportion of overland (quick) and subsurface (slow) flow. Subsurface flow increases gradually together with increasing the depth of thawed ground. Domination of overland flow during snowmelt alters by domination of subsurface flow at the middle of the warm period, then the proportion of the surface flow and the subsurface one depends

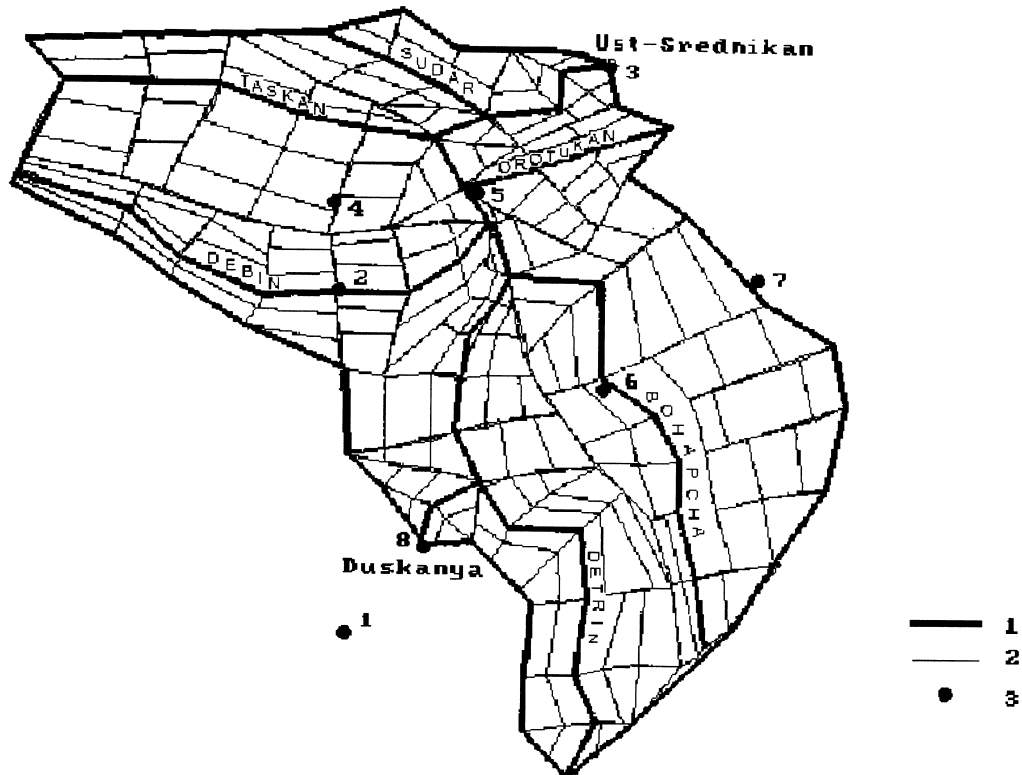


Fig. 8. Finite-element schematisation of the Upper Kolyma River basin: 1-channel system; 2-boundaries of the finite elements; 3-meteorological stations.

mainly on the rainfall characteristics and the catchment slope. When the depth of thawed ground reaches 0.3–0.5 m and the horizontal hydraulic conductivity near the frozen layer becomes small, the subsurface flow was observed only at large rainfalls.

4. A model of runoff generation in the Upper Kolyma River basin

On the basis of analysis of hydrometeorological data in the Upper Kolyma River basin and the literature in the permafrost hydrology, we accepted the following general scheme of runoff generation. The snowmelt water, first of all, fills up the free storage capacity in topographic depressions, the peat mats and the ground where this water freezes. It is assumed that the basin storage capacity is statistically distributed over the basin and the mathematical expectation of

this capacity before snowmelt depends only on water balance of the ground in the antecedent summer–autumn period (before snowmelt ground is deeply frozen). Excess snowmelt and rainfall water over the free storage capacity forms overland flow. Ice melting and evaporation of soil moisture begin at the snow free areas of the river basin. The melt of ice in the ground and in the depressions produces the subsurface flow and increases the basin storage capacity. The subsurface flow occurs above the frozen layer of the ground. The water retained by the capillary forces does not take part in subsurface flow. The infiltration of rainfall into the ground is quick and does not depend on the ground moisture conditions.

The major components of the developed distributed model of the Upper Kolyma River basin are schematically shown in Fig. 7.

Let us consider the description of separate processes and the construction of the whole runoff

generation model for the Upper Kolyma River basin.

4.1. Modelling of overland, subsurface and channel flow

To model overland, subsurface and channel flow, a finite-element schematisation of the Upper Kolyma River basin has been applied (Fig. 8). The channel river system is represented by the main channel of the Kolyma River and by six tributaries. The largest of them are the Bochapcha River (the catchment area is 13,800 km²), and the Taskan River (the catchment area is 11,200 km²). The channel system is divided into 44 reaches (finite elements) taking into account the topography and the river network structure; the basin area is separated on strips, adjacent to the channel finite elements and along which one-dimensional flow to river channels is assumed. The strips also are divided into finite elements with different characteristics of topography.

The kinematic wave equations are applied to describe the overland and channel flow. To account for the subsurface flow, the following equations are used (Kuchment et al., 1990)

$$(\theta_m - \theta_f) \frac{\partial h}{\partial t} + \frac{\partial q}{\partial x} = G \quad (1)$$

$$q = K(H) i_0 h$$

where θ_m is the volumetric porosity of ground, θ_f the field capacity of ground, h the subsurface flow depth, q the subsurface flow discharge, i_0 the slope of the layer with subsurface flow, G the input of rainfall and melted water per area unit of this layer, $K(H)$ the horizontal hydraulic conductivity and H the depth of thawed ground.

It is assumed that the horizontal hydraulic conductivity exponentially decays with the depth H as

$$K = K_0 \exp(-\varphi H), \quad (2)$$

where K_0 is the horizontal hydraulic conductivity near the ground surface and φ is the parameter of decay.

Numerical integration of the equations which describe the overland, subsurface and channel flow has been carried out using the finite-element method (Kuchment et al., 1983; Kuchment et al., 1996).

4.2. Snow cover formation and snowmelt

To calculate the characteristics of snow cover during snowmelt, the system of vertically averaged equations of snow processes in a point has been applied (Kuchment and Gelfan, 1996). The system includes the description of temporal change of the snow depth, content of ice and liquid water, snow density, snowmelt, sublimation, re-freezing melt water, snow metamorphism and is written as follows:

$$\frac{dH_s}{dt} = \rho_w [X_s \rho_0^{-1} - (S + E_s)(\rho_i I_s)^{-1}] - V \quad (3a)$$

$$\frac{d}{dt}(\rho_s I_s H_s) = \rho_w (X_s - S - E_s) + S_i \quad (3b)$$

$$\frac{d}{dt}(\rho_w w_s H_s) = \rho_w (X_l + S - R_s) - S_i \quad (3c)$$

where H_s is the snow depth, I_s and w_s are the volumetric content of ice and liquid water, respectively; X_s and X_l are the snowfall rate and the rainfall rate, respectively (it is assumed that if the temperature of air $T_a \geq 0^\circ\text{C}$ only rainfall occurs and if $T_a < 0^\circ\text{C}$ only snowfall occurs); S is the snowmelt rate; ρ_w , ρ_i , ρ_s and ρ_0 are the density of water, ice, snowpack, and new snow; E_s is the rate of snow evaporation, S_i is the rate of re-freezing melt water in snow, R_s is the meltwater outflow from snowpack and V is the compression rate.

The snowmelt rate S is determined as (Kuusisto, 1984)

$$S = \beta \rho_s T_a \quad (4)$$

where β is an empirical coefficient.

The meltwater outflow is determined as (Motovilov, 1993)

$$R_s = \begin{cases} R_0 + S, & w_s = w_{\max} \\ 0, & w_s < w_{\max} \end{cases} \quad (5)$$

where $R_0 = X_l + S - E_s - w_{\max}(dH_s/dt)$, and w_{\max} is the maximum liquid water-retention capacity calculated as (Kuchment et al., 1983)

$$w_{\max} = \frac{0.11 - 0.11 \rho_i I_s \rho_w^{-1}}{1.11 - 0.11 \rho_w \rho_i^{-1} I_s^{-1}} \quad (6)$$

It is assumed that the rate of re-freezing $S_i = K_i |T_a|^{0.5}$ while $K_i = 5.8 \times 10^{-8} \text{ m s}^{-1} \text{ }^\circ\text{C}^{-1}$ (Motovilov, 1993).

The compression rate V is determined as

$$V = 0.5\xi\rho_s \exp(0.08T_a - \zeta\rho_s)H_s^2 \quad (7)$$

where $\xi = 2.7 \times 10^{-7} \text{ m}^2 \text{ s}^{-1} \text{ kg}^{-1}$ and $\zeta = 2.1 \times 10^{-4} \text{ m}^3 \text{ kg}^{-1}$ (Anderson, 1976).

According to the data of measurements at the Kolyma water balance station, the rate of snow evaporation E_s is close to 1.0 mm day^{-1} (see Fig. 6)

The numerical integration of Eqs. (3a)–(3c) has been carried out using an explicit finite-difference scheme described by Motovilov (1993).

To take into account spatial mosaic variability of the snowpack characteristics before melting, the Upper Kolyma River basin was divided into 16 approximately equal subareas corresponding to the available snow course network. It was assumed that the spatial stochastic variations of the snow water equivalent within each subarea can be described by log-normal statistical distribution (see, for example, (Gottschalk and Jutman, 1979; Killingtveit and Sand, 1991). The mean values of the snow water equivalent needed for the construction of this distribution for each subarea were taken to be equal to the snow water equivalent at the corresponding snow course; standard deviations of snow water equivalent for each subarea were equated to the standard deviation estimated for the whole basin. The snowmelt rate was calculated using the system (3) for each finite element taking into account both mosaic and stochastic variations of snow water equivalent. It was assumed while calculating that the initial (before melting) snow density was equal to measured one; the initial snow depths were obtained by dividing the measured values of snow water equivalent on the snow density.

4.3. Thawing of the ground

The movement of the front of ground thawing is described by the following equations (Kuchment, 1980):

$$C_{\text{uf}} \frac{\partial T}{\partial t} = \frac{\partial}{\partial z} \left(\lambda_{\text{uf}} \frac{\partial T}{\partial z} \right), \quad 0 < z < H(t) \quad (8a)$$

$$C_{\text{f}} \frac{\partial T}{\partial t} = \frac{\partial}{\partial z} \left(\lambda_{\text{f}} \frac{\partial T}{\partial z} \right), \quad H(t) < z < L \quad (8b)$$

$$\lambda_{\text{uf}} \frac{\partial T}{\partial z} \Big|_{z=H-0} = \lambda_{\text{f}} \frac{\partial T}{\partial z} \Big|_{z=H+0} + \chi \frac{\rho_{\text{i}}}{\rho_{\text{w}}} I \frac{dH}{dt} \quad (8c)$$

$$T(0, t) = T_{\text{a}}(t); \quad T(H, t) = 0; \quad (8d)$$

$$T(L, t) = T_{\text{L}}; \quad T(z, 0) = T(z)$$

where $H(t)$ is the depth of thawed ground at time t , $T(z, t)$ the ground temperature at depth z and time t , λ_{f} and λ_{uf} are the thermal conductivities of frozen and thawed ground, respectively, C_{f} and C_{uf} are the heat capacities of frozen and thawed ground, respectively, χ is the latent heat of ice fusion, I the volumetric content of ice in the ground and L the depth of the ground where the ground temperature can be considered as constant equated T_{L} (L was taken to be equal to 3 m).

The thermal conductivities ($\text{J m}^{-1} \text{ s}^{-1} \text{ }^\circ\text{C}^{-1}$) were calculated as (Ivanov and Gavrilov, 1965; Kuchment et al., 1990)

$$\lambda_{\text{uf}} = 1.1 \log \frac{\theta}{\rho_{\text{g}}} + 1.8 \quad (9)$$

$$\lambda_{\text{f}} = 1.3\lambda_{\text{uf}} \quad (10)$$

where θ is the volumetric content of liquid water in the ground and ρ_{g} is the density of ground.

The heat capacities of the frozen and thawed ground were calculated as weighted-average values of the specific heat capacities of ground matrix C_{m} , liquid water C_{w} and ice C_{i} (Kuchment et al., 1983):

$$C_{\text{f}} = \rho_{\text{m}}C_{\text{m}}(1 - \theta_{\text{m}}) + \rho_{\text{i}}C_{\text{i}}I \quad (11)$$

$$C_{\text{uf}} = \rho_{\text{m}}C_{\text{m}}(1 - \theta_{\text{m}}) + \rho_{\text{w}}C_{\text{w}}\theta \quad (12)$$

where ρ_{m} is the density of the ground matrix.

An implicit four-point finite difference scheme was used for the numerical integration of the equations of thermal conductivity (8a) and (8b); the corresponding difference equations were solved by the double-sweep method (Samarsky, 1983).

4.4. Retention of melt and rainfall water by basin storage and formation of runoff input on contributing basin areas

It is assumed that the spatial distribution of the free storage capacity P is exponential, i.e.

$$f(P) = \frac{1}{\bar{P}} \exp\left(-\frac{P}{\bar{P}}\right) \quad (13)$$

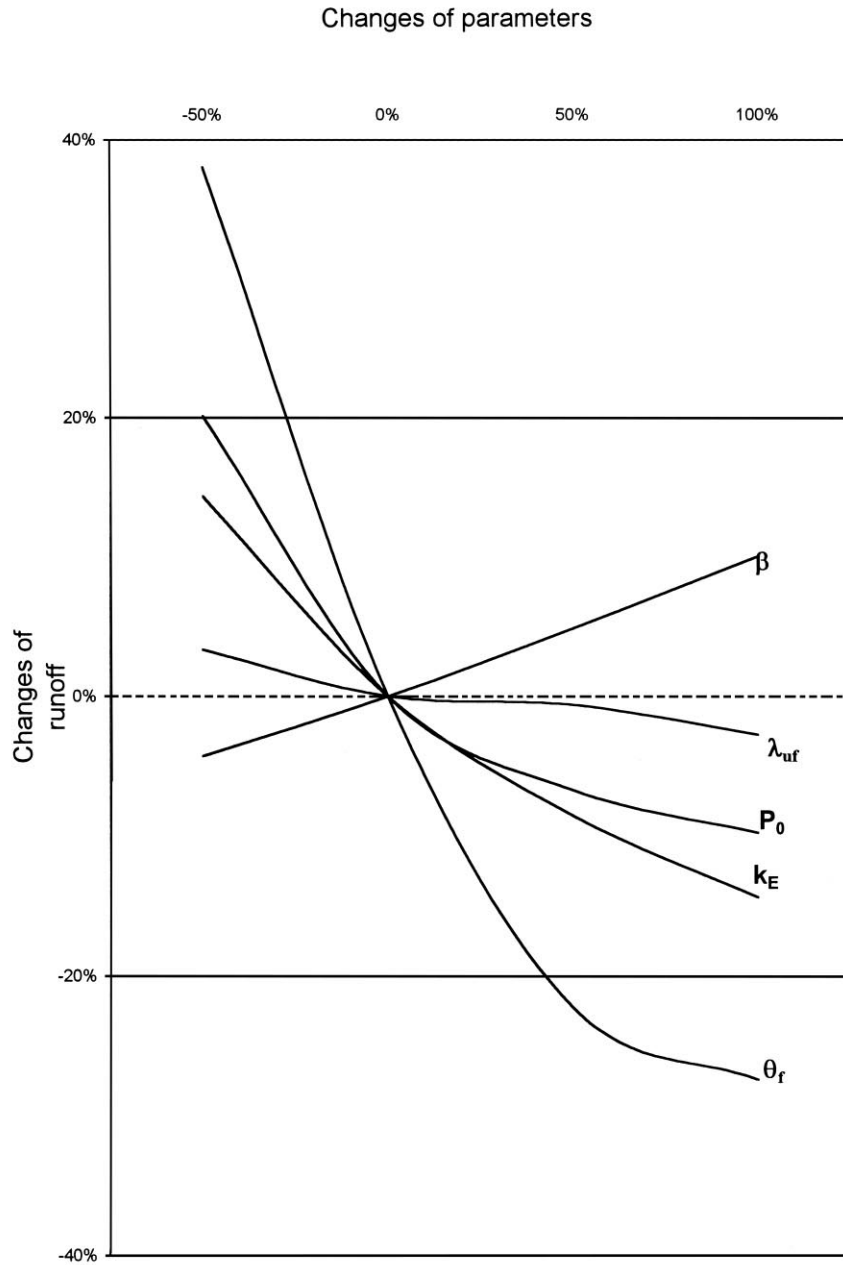


Fig. 9. Sensitivity of the calculated runoff to changes of the main parameters of the model.

where $f(P)$ is the probability distribution function and \hat{P} is the mathematical expectation of P (or the maximum possible retention).

Then the sum retention of water D by this basin storage up to time t after the beginning of snowmelt

can be determined as

$$D = \int_0^R [1 - F(P)] dP = \hat{P} \left[1 - \exp\left(-\frac{R}{\hat{P}}\right) \right] \quad (14)$$

where $F(P) = \int_0^P f(P) dP = 1 - \exp(-P/\hat{P})$ and R is

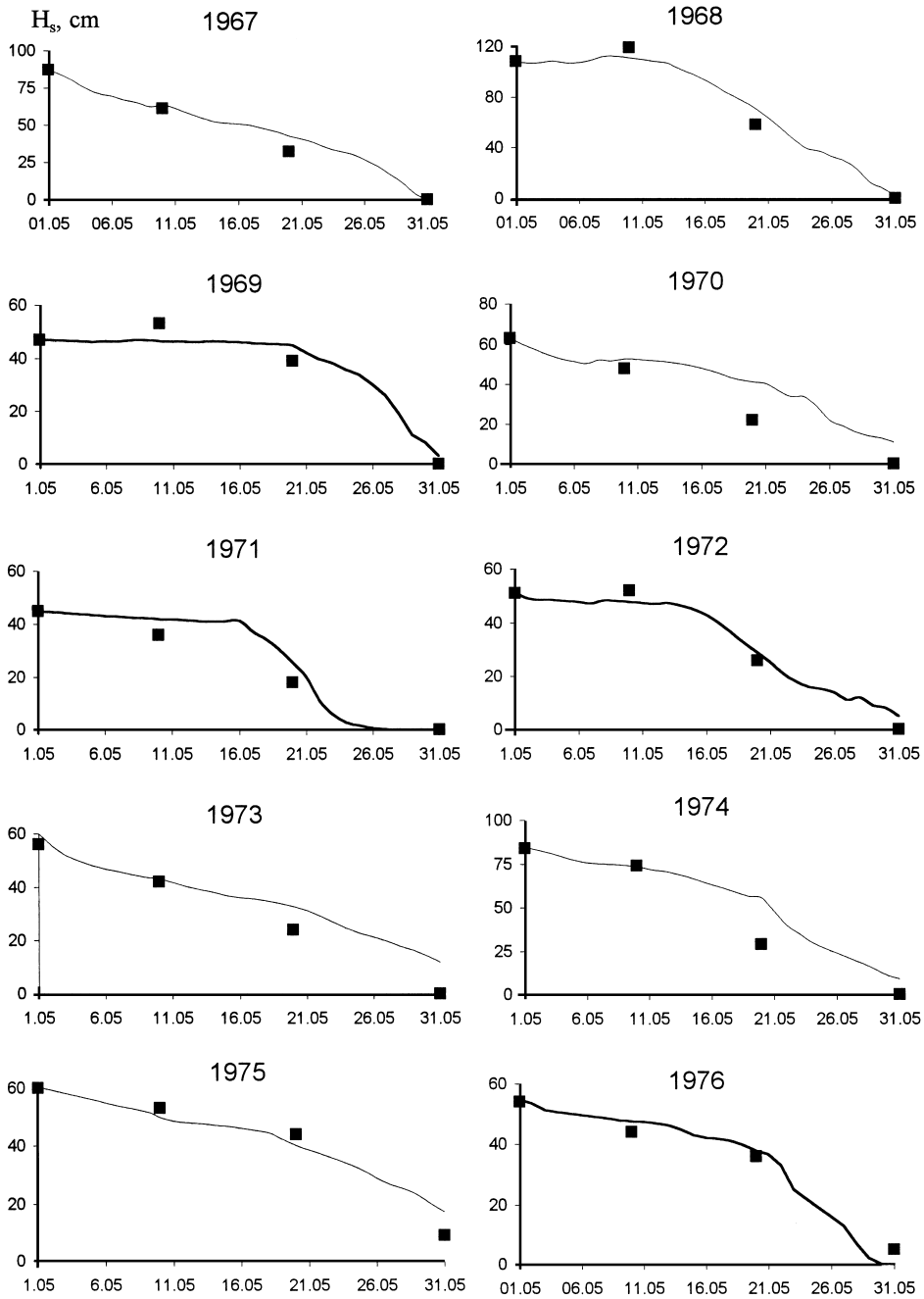


Fig. 10. Comparison between measured (squares) and calculated (lines) snow depths.

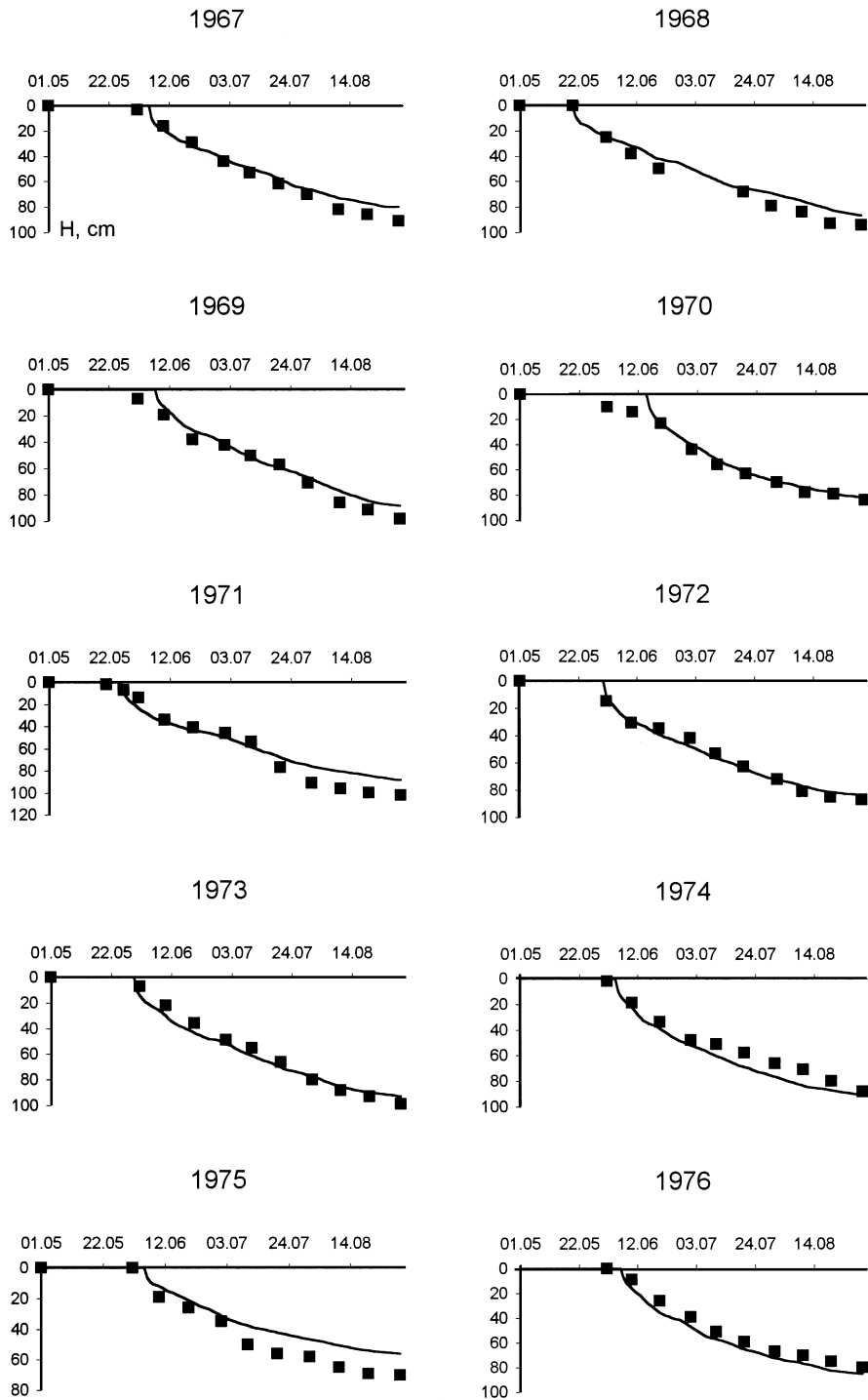


Fig. 11. Comparison between measured (squares) and calculated (lines) depth of thawed ground.

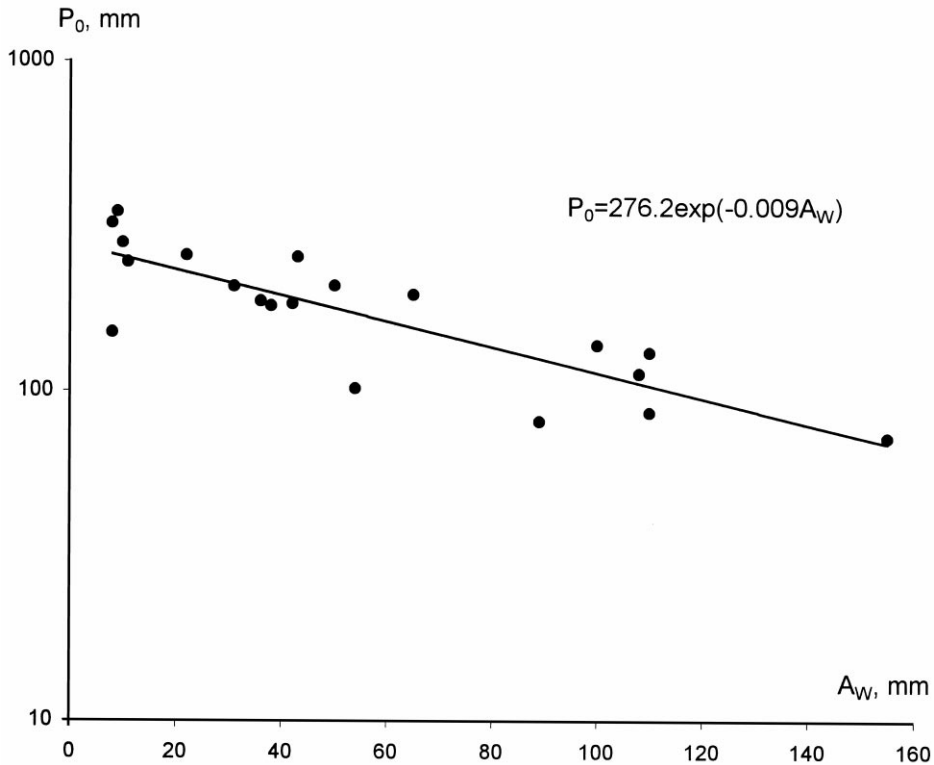


Fig. 12. Relation between free storage capacity before snowmelt and antecedent wetness index.

the sum input of melt and rainfall water on basin area up to time t .

The excess of water contribution over the retention forms the overland flow input.

The basin storage capacity begins to increase after the start of icemelt and $\hat{P} = P_0 + d_W$, where P_0 is the free storage capacity before snowmelt, and d_W is the additional capacity which is free as a result of icemelt to the time t .

The value of d_W is calculated as

$$d_W = (\theta_m - \theta)(H - h) \quad (15)$$

Assuming that the ground retains the moisture only by the capillary forces and the moisture excess over the field capacity θ_f forms the subsurface flow input G , we obtain the equations of the ground moisture balance in the thawed layer H in the following form:

$$\frac{d}{dt}(\theta H) = \frac{dD}{dt} - E + I \frac{\rho_i}{\rho_w} \frac{dH}{dt} \quad \text{for } \theta < \theta_f \quad (16)$$

$$G = \frac{dD}{dt} - E + I \frac{\rho_i}{\rho_w} \frac{dH}{dt} \quad \text{for } \theta \geq \theta_f \quad (17)$$

where E is the evaporation rate.

The evaporation rate is determined as

$$E = k_E d_a \frac{\theta}{\theta_f} \quad (18)$$

where k_E is an empirical coefficient and d_a is the air humidity deficit.

4.5. Calibration of the model, its verification and discussion of results

To calibrate and to verify the model of runoff generation on the Upper Kolyma River basin, daily hydrometeorological data measurements from 1 May to 31 August during 10 years (1967–1976) were used. The meteorological data included records at eight sites (see Fig. 8). The initial spatial distribution of

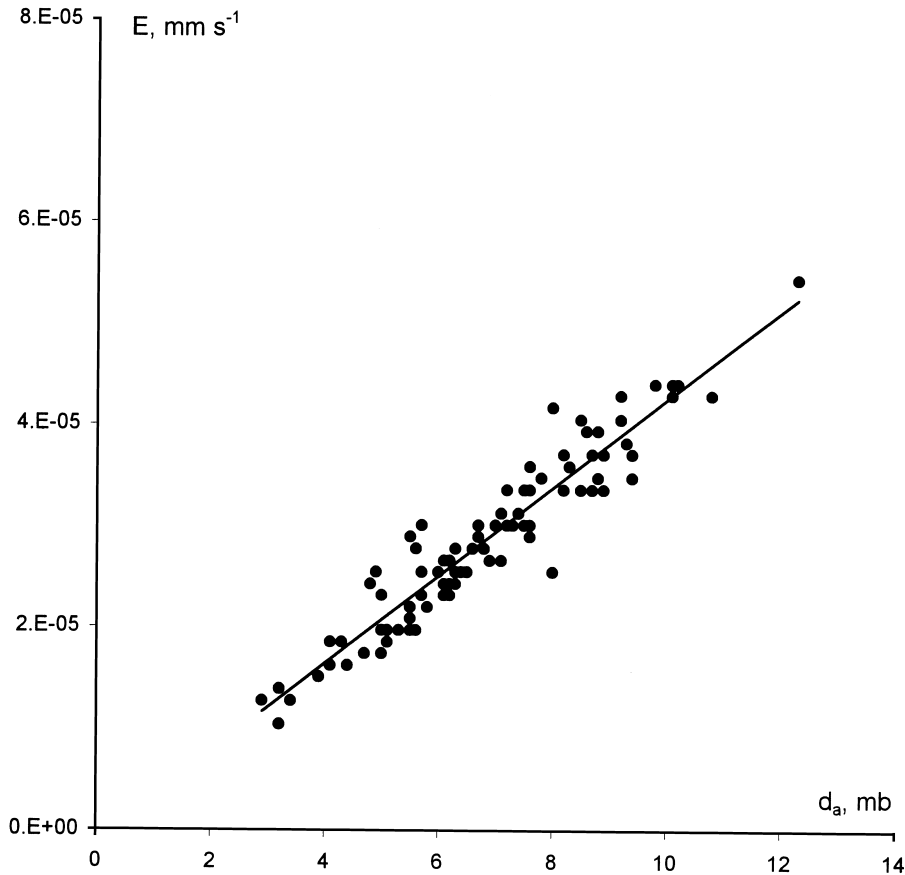


Fig. 13. Relation between measured evaporation and air humidity deficit.

the snow water equivalent was assigned using snow measurements for 16 snow courses.

A set of numerical experiments had been carried out to estimate the sensitivity of the runoff hydrographs to change of different parameters of the model before the calibration. The sensitivities of the runoff hydrographs for 10 seasons to five main parameters are shown in Fig. 9. It has been determined that the parameters θ_f and k_E (see formulae (16)–(18)) are the most important. These two parameters control accumulation and discharge of water in the ground during the entire period of runoff generation. The parameter β controls snowmelt and has a significant influence on overland flow but during a short period. The parameter P_0 strongly influences on the runoff hydrograph form at both snowmelt and rainfall input.

The influence of the routing parameters (Manning's

coefficients of roughness for the slope surface n_s and the river channels n_r as well as the horizontal hydraulic conductivity K_0) is relatively small because of large variability of the slopes and the linear characteristics of the river basin. The initial values of these parameters have been changed within narrow range in the calibration process.

A part of the parameters of the model were determined on the basis of the measurements on the Kolyma water balance station during periods of 1965–1984.

According to the available measurements at the Kolyma water balance station, the following values of the ground constants have been assigned: the density of ground $\rho_g = 1520 \text{ kg m}^{-3}$, the volumetric porosity of ground $\theta_m = 0.4$, the density of the ground matrix $\rho_m = 2600 \text{ kg m}^{-3}$, the specific heat capacity

Table 1
Parameters of the model of runoff generation in the Upper Kolyma River basin

Mathematical symbol	Physical meaning	Numerical value
<i>Constants measured in the Kolyma water balance station</i>		
ρ_g	Density of ground	1520 kg m ⁻³
ρ_m	Density of the ground matrix	2600 kg m ⁻³
θ_m	Volumetric porosity of ground	0.4
C_m	Specific heat capacity of ground matrix	1100 J kg ⁻¹
φ	Decay of hydraulic conductivity with depth of active layer	3.1 m ⁻¹
<i>Parameters calibrated using Kolyma water balance station observation data</i>		
P_0	Free storage capacity before snowmelt	Fig. 12
β	Empirical coefficient (formula 4)	$1.6 \times 10^{-10} \text{ m}^4 \text{ }^\circ\text{C}^{-1} \text{ kg}^{-1} \text{ s}^{-1}$
<i>Parameters calibrated using measured hydrographs of Kolyma River</i>		
θ_f	The field capacity of the ground	0.29
n_s	Manning's coefficient of roughness for the slope surface	0.11 s m ^{-1/3}
n_r	Manning's coefficient of roughness for the river channels	0.07 s m ^{-1/3}
K_0	horizontal hydraulic conductivity	0.1 m s ⁻¹
k_E	Empirical coefficient (formula 18)	$3.8 \times 10^{-9} \text{ m mb}^{-1} \text{ s}^{-1}$

of ground matrix $C_m = 1100 \text{ J kg}^{-1}$, the value of the parameter φ in formula (2) equalled 3.1 m^{-1} .

The value of β (see formula (4)) has been calibrated using snow measurement data at the Kolyma water balance station in 1967–1970 and has been found to be $1.6 \times 10^{-10} \text{ m}^4 \text{ }^\circ\text{C}^{-1} \text{ kg}^{-1} \text{ s}^{-1}$. The model (3)–(7) of snow cover formation and snowmelt has been tested against snow measurements in 1971–1976. As can be seen from Fig. 10, the calculated snow depths are in good agreement with the measurements of snow depths.

The model (8)–(12) of ground thawing has been tested against measurements in 1967–1976. As can be seen from Fig. 11, the calculated depth of thawed ground are in good agreement with those measured.

The parameters P_0 (free storage capacity before snowmelt; see below formula (14)) were fitted for each snowmelt flood using the data 20 years (1965–1984) water balance measurements at the Kontaktny River basin and the relation between P_0 and the antecedent wetness index A_W were constructed (Fig. 12). The index A_W was calculated as a difference between the sum of the measured precipitation and the sum of the evaporation for the period from July to September. The dependence shown in Fig. 12 was applied for determination of P_0 .

To assign the coefficient k_E (see formula (18)), the relation between the evaporation and air humidity deficit both measured at the Kontaktny basin was

used (Fig. 13). This relation is given the value of k_E equalled $4.3 \times 10^{-9} \text{ m mb}^{-1} \text{ s}^{-1}$. This value has been taken as the first approximation for calibration of k_E .

The calibration of the whole model of runoff generation on the Upper Kolyma River basin was performed by comparison of the measured and calculated runoff discharges at the outlet of the river basin during periods of 1967–1970. The following values of the calibrated parameters were obtained: $k_E = 3.8 \times 10^{-9} \text{ m mb}^{-1} \text{ s}^{-1}$, $\theta_f = 0.29$; $K_0 = 0.1 \text{ m s}^{-1}$; $n_s = 0.11 \text{ s m}^{-1/3}$ $n_r = 0.07 \text{ s m}^{-1/3}$. The list of the parameters utilised by the model is shown in Table 1.

Comparison of the measured and the calculated

Table 2
Measured and calculated runoff characteristics

Year	Runoff yield (mm)		Maximum discharge (m ³ s ⁻¹)	
	Measured	Calculated	Measured	Calculated
1976	143	128	4770	5297
1975	180	167	4740	5615
1974	171	165	5430	6423
1973	109	101	3540	4084
1972	176	190	5560	5070
1971	146	125	4150	3996
1970	190	166	3810	4064
1969	194	190	7060	7116
1968	248	250	10200	9947
1967	234	243	6100	6612

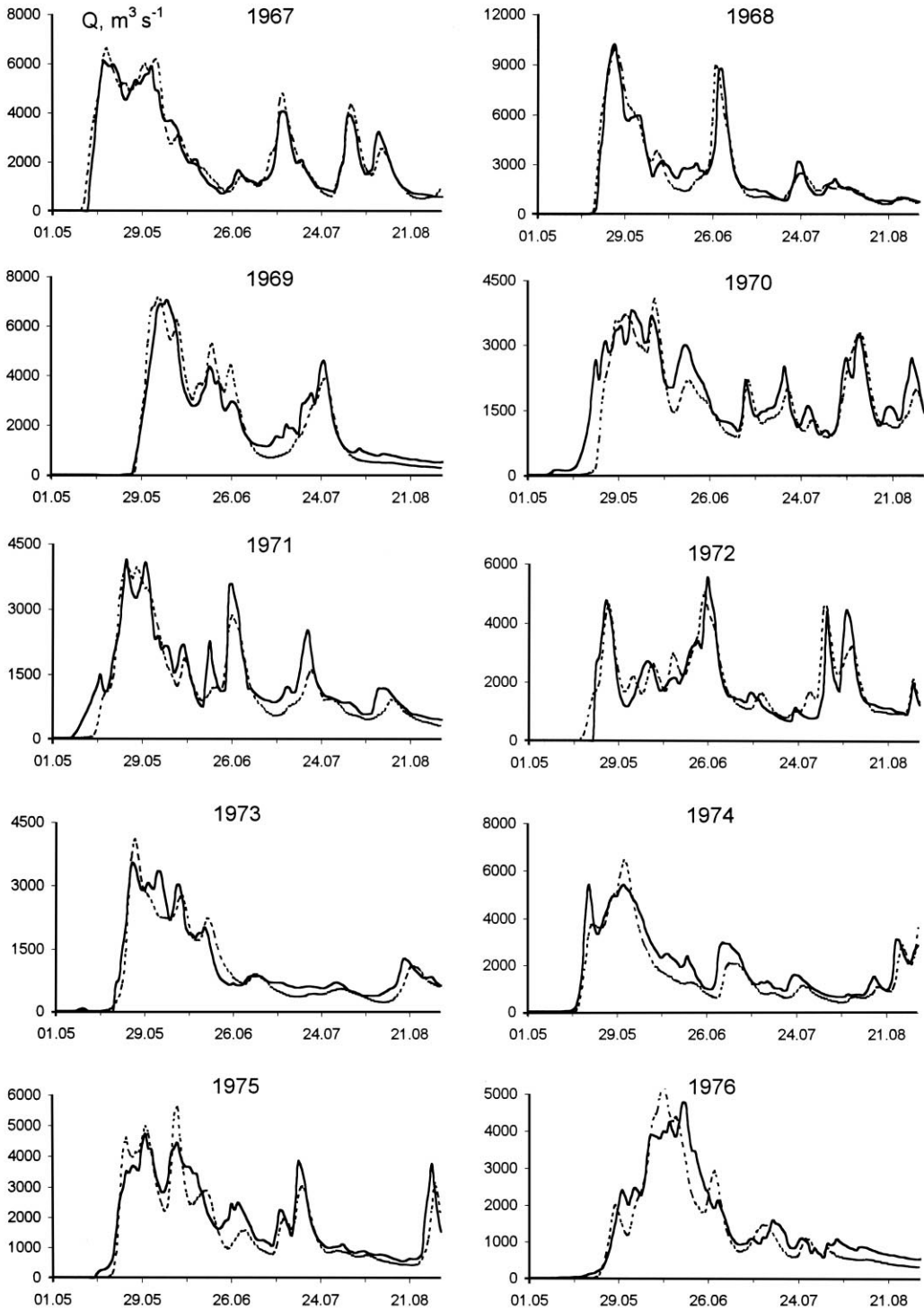


Fig. 14. Comparison between measured (continuous line) and calculated (dashed line) hydrographs.

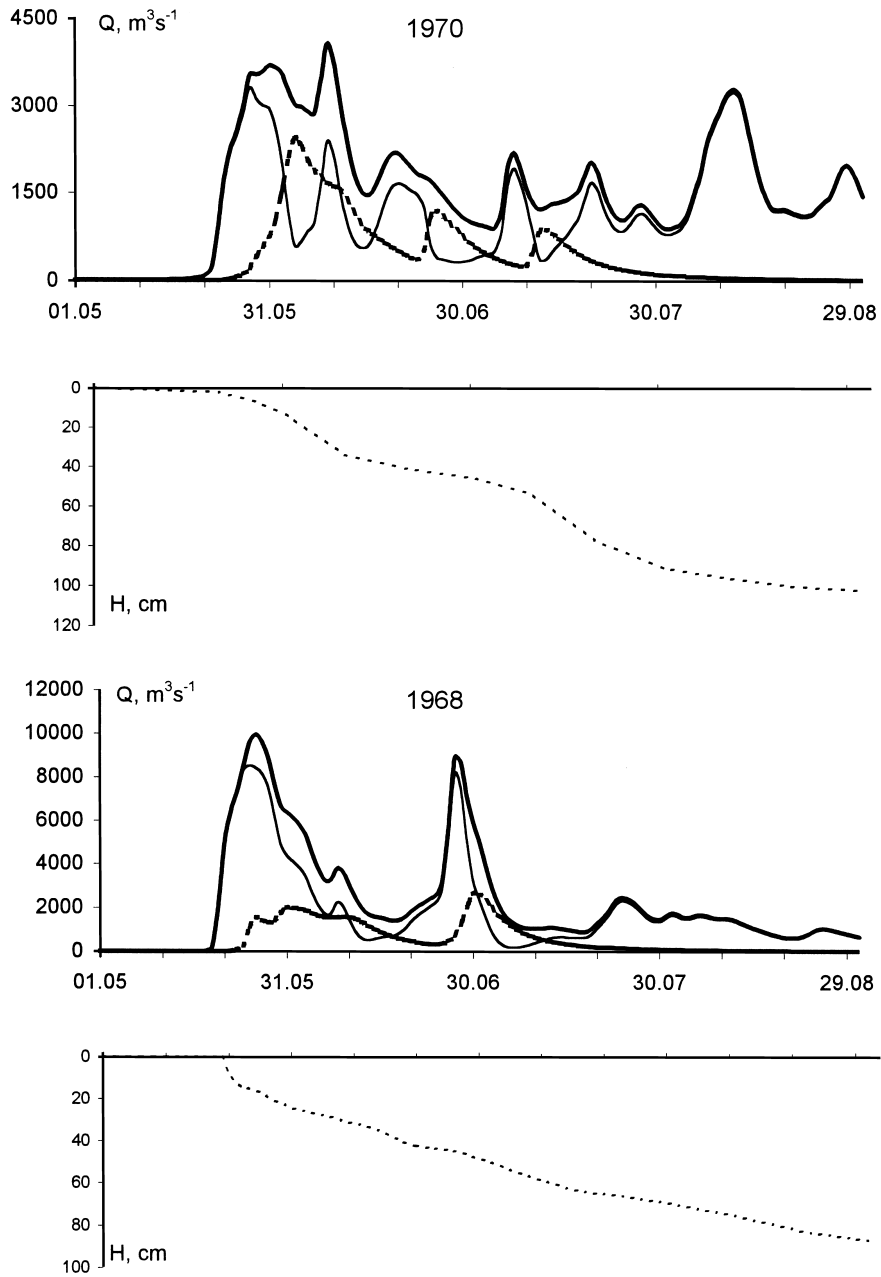


Fig. 15. Streamflow discharges (bold continuous line), surface and subsurface contributions to streamflow (fine continuous line and bold dashed line, respectively), and depth of the active layer of ground (fine dashed line).

Table 3
Calculated water balance of the Upper Kolyma River basin (from 1 May–31 August)

Year	Snowmelt plus rainfall (mm)	Icemelt minus storage detention (mm)	Evaporation (mm)	Surface flow (mm)		Subsurface flow (mm)
				During snowmelt period	After snowmelt period	
1976	197	107	176	38	34	56
1975	227	61	121	76	52	39
1974	188	96	119	61	74	30
1973	116	129	144	35	22	44
1972	172	114	99	44	52	91
1971	173	98	125	51	42	53
1970	217	110	161	58	41	67
1969	202	138	150	30	68	92
1968	279	131	162	130	81	37
1967	254	95	106	136	52	55
Average (mm)	202.5	107.9	136.3	65.9	51.8	56.4

hydrographs for all 10 years is given in Fig. 14 and Table 2.

The standard error of the calculated runoff hydrographs is $482 \text{ m}^3 \text{ s}^{-1}$ (the standard deviation of the measured hydrographs is $1434 \text{ m}^3 \text{ s}^{-1}$). The standard error of the calculated peak discharges is $490 \text{ m}^3 \text{ s}^{-1}$. The largest relative error of the peak discharges is 18% (for 1974) and the largest relative errors of the runoff volume are 14% (for 1971) and 13% (for 1970).

The analysis of the water balance components for all 10 years has revealed that underestimation of runoff volumes for 1970 and 1971 and overestimation of runoff volumes for 1972 can be explained mainly by errors in determination of P_0 from the relationship in Fig. 14. As can be seen from the analysis of calculated water balance components (Table 3), the icemelt water can give about 50% of rainfall and snowmelt total input, however, the most part of this water evaporates or detains in the ground storage capacity. The surface flow volume is two times more than the subsurface one; however, after snowmelt the contributions of the surface and the subsurface flows are approximately equal. The examples of the temporal change of these contributions are shown in Fig. 15. As can be seen from these graphs, the subsurface flow decreases with increasing the thawed layer depth. Obtained estimations of the surface and the subsurface contributions into the total flow are close to estimations obtained for the same region using experimental data (Gopchenko, 1969).

5. Conclusions

A physically based distributed model of runoff generation in permafrost regions has been proposed. Main difference of this model from models of runoff generation for regions with moderate climate is a small role of infiltration of water into soil and a larger dependence of runoff losses on the depth of thawed ground. The thaw of the frozen ground significantly increases the water input and the water storage capacity and changes the ratio between surface and subsurface flow. Application of the proposed model to the Upper Kolyma River basin has shown that the model simulates satisfactory these peculiarities as well as the other processes of runoff generation in cold regions. The problem of using the proposed model is availability of data needed to assign or to calibrate the model parameters. The results obtained for the Kolyma River basin enables us to assume that for many river basins most parts of used parameters change in relatively narrow ranges and can be considered as regionally common. Some of these parameters can be determined using the measurements on a small area inside of the river basin or on the basis of the literature data.

Acknowledgements

The present work was carried out as part of a

research project supported by the Russian Foundation of Fundamental Researches (Grant N96-05-65755).

References

- Anderson, E., 1976. A point energy and mass balance model of snow cover. NOAA Tech. Memo, NWS-Hydro, vol. 19, 151 pp.
- Gopchenko, E.D., 1969. Experimental investigations of rainfall runoff generation in permafrost region. *J. Meteorol., Climatol. Hydrol.* 5, 218–223 (in Russian).
- Gottschalk, L., Jutman, T., 1979. Statistical analysis of snow survey data. SMHI Report. No. RHO-20, Norrköping, Sweden, 41 pp.
- Grigoriev, V.Yu., Sokolov, B.L., 1994. Northern hydrology in the former Soviet Union. In: Prowse, T.D., Ommanney, C.S.L., Watson, L.E. (Eds.), *Northern Hydrology: International Perspectives*, NHRI Science Rep. No. 3. National Hydrology Research Institute, Environment Canada, Saskatoon, Saskatchewan, pp. 147–179.
- Ivanov, N.S., Gavrilov, R.I., 1965. *Thermophysical Properties of Rocks*. Nauka, Moscow (in Russian).
- Killingtveit, Å., Sand, K., 1991. On areal distribution of snowcover in a mountainous area. In: Prowse, T.D., Ommanney, C.S.L. (Eds.), *Northern Hydrology: Selected Perspectives*, NHRI Symp. No. 6. National Hydrology Research Institute, Environment Canada, Saskatoon, Saskatchewan, pp. 189–204.
- Kuchment, L.S., Gelfan, A.N., 1996. The determination of the snowmelt rate and meltwater outflow from a snowpack for modelling river runoff generation. *J. Hydrol.* 179, 23–36.
- Kuchment, L.S., Demidov, V.N., Naden, P.S., Cooper, D.M., Broadhurst, P., 1996. Rainfall-runoff modelling of the Ouse basin, North Yorkshire: an application of a physically based distributed model. *J. Hydrol.* 181, 323–342.
- Kuchment, L.S., Motovilov, Yu.G., Nazarov, N.A., 1990. Sensitivity of the Hydrological Systems. Nauka, Moscow (in Russian).
- Kuchment, L.S., Demidov, V.N., Motovilov, Yu.G., 1983. *River Runoff Formation (Physically-based Models)*. Nauka, Moscow (in Russian).
- Kuchment, L.S., 1980. *Models of the River Runoff Generation Processes*. Hydrometeoizdat, Leningrad (in Russian).
- Kuusisto, E., 1984. *Snow Accumulation and Snowmelt in Finland*. Publ. Water Research Institute, Helsinki.
- Motovilov, Yu.G., 1993. Modelling snowpack formation and snowmelt. In: Kuchment, L.S., Muzylev, E.L. (Eds.), *Modelling the Hydrological Cycle of River Basins*. Nat Geoph Committee Publ, Moscow, pp. 9–37 (in Russian).
- Pomeroy, J.W., Marsh, P., Gray, D.M., 1997. Application of a distributed blowing snow model to the Arctic. *Hydrol. Processes* 11, 1451–1464.
- Pomeroy, J.W., Jones, H.G., 1996. Wind-blown snow: sublimation, transport and changes to polar snow. In: Wolff, E., Bales, R.C. (Eds.), *Chemical Exchange between the Atmosphere and Polar Snow*. NATO ASI Series I, vol. 43. Springer, Berlin, pp. 453–489.
- Price, J.S., Woo, Ming-K., 1988. Studies of a subarctic coastal marsh. *J. Hydrol.* 103, 275–292.
- Roulet, N.T., Woo, Ming-K., 1988. Runoff generation in a low arctic drainage basin. *J. Hydrol.* 101, 213–226.
- Roulet, N.T., Woo, Ming-K., 1986. Hydrology of a wetland in the continuous permafrost region. *J. Hydrol.* 89, 73–91.
- Samarsky, A.A., 1983. *Theory of Finite-differences Schemes*. Nauka, Moscow (in Russian).
- Sokolov, B.L., 1975. *Naleds and River Runoff*. Hydrometeorological Publ, Leningrad (in Russian).
- Woo, Ming-K., 1990. Permafrost hydrology. In: Prowse, T.D., Ommanney, C.S.L. (Eds.), *Northern Hydrology: Canadian Perspectives*, NHRI Science Rep. No. 1. National Hydrology Research Institute, Environment Canada, Saskatoon, Saskatchewan, pp. 63–76.